

A peroxochromium complex, $\text{Tp}^{\text{iPr}_2}\text{Cr}(\text{O}_2)_2$, obtained by oxidative dehydrative condensation between a dihydroxochromium complex and H_2O_2 [Tp^{iPr_2} = hydrotris(3,5-diisopropylpyrazolyl)borato]†

Ken-ichiro Sugawara, Shiro Hikichi*‡ and Munetaka Akita*

Chemical Resources Laboratory, Tokyo Institute of Technology, 4259 Nagatsuta, Midori-ku, Yokohama 226-8503, Japan

Received 13th August 2003, Accepted 2nd September 2003

First published as an Advance Article on the web 18th September 2003

Synthesis of a peroxochromium complex containing the Tp^{iPr_2} [hydrotris(3,5-diisopropylpyrazolyl)borato] ligand has been attempted by (i) dehydrative condensation between hydroxochromium complexes and H_2O_2 and (ii) oxidative addition to a Cr(II) species. As a result, a diperoxochromium(v) complex, $\text{Tp}^{\text{iPr}_2}\text{Cr}(\text{O}_2)_2$, is obtained by oxidative dehydrative condensation of the dimeric (dihydroxo)(aquo)chromium(III) complex, $[\text{Tp}^{\text{iPr}_2}\text{Cr}(\text{OH})_2(\text{OH}_2)]_2$, with H_2O_2 , whereas O_2 -oxidative addition to Cr(II) species affords Cr(III) species or dinuclear $\text{Tp}^{\text{iPr}_2}\text{Cr}$ species bridged by chromate (CrO_4) or dichromate ions (Cr_2O_7). The preparations of the starting complexes and oxidation reactions by the diperoxo complex are also described.

Introduction

Dioxygen–transition metal adducts play pivotal roles in organic and biological oxidative transformations as well as O_2 -transport in living systems.¹ In our laboratory systematic synthetic study of dioxygen complexes has been carried out by using the versatile hydrotrispyrazolylborato ligands (Tp^{R}), facially coordinating tripodal N_3 -donors.^{2–4} As a result, a series of dioxygen complexes with first- and second-row metals has been prepared and characterized successfully, and the central metal has been extended to early transition metal including vanadium⁵ and chromium.⁶ In a previous paper we reported synthesis of chlorochromium(II) complexes with the Tp^{iPr_2} ligand⁶ and their unique behavior as a reductant; one-electron transfer to organic substrates associated with formation of chromium(III) species causes C–Cl homolysis of organic chlorides and reductive coupling of benzaldehyde.⁶

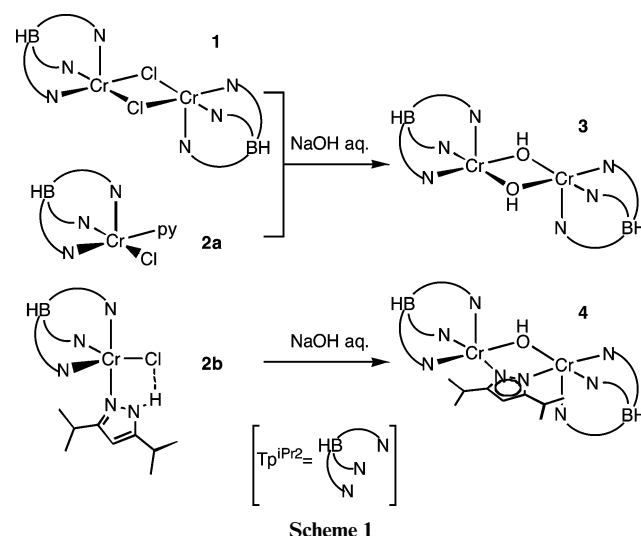
Herein we will describe the results of attempts to prepare a peroxochromium complex bearing the Tp^{iPr_2} ligand,⁴ a new member of $\text{Tp}^{\text{R}}\text{M}-\text{O}_2$ adducts, starting from the $\text{Tp}^{\text{iPr}_2}\text{Cr}(\text{II})$ precursors.⁶ The reduction feature of the Cr(II) species mentioned above prompted us to examine O_2 -oxidative addition, which was a promising route to peroxo complexes. Furthermore hydroxo complexes derived from the chloro complexes were subjected to dehydrative condensation with H_2O_2 , which was also recognized as a versatile synthetic method for dioxygen complexes.² As a result of the present study, a desired peroxo chromium complex, $\text{Tp}^{\text{iPr}_2}\text{Cr}^{\text{V}}(\text{O}_2)_2$, was obtained *via* oxidative dehydrative condensation of a hydroxochromium(III) complex with H_2O_2 . In contrast to oxochromium ($\text{Cr}=\text{O}$) species, which are versatile oxidizing reagents of organic substrates, peroxochromium species have not been studied in a systematic manner,⁷ while intriguing aspects of the chemistry of Cr– O_2 adducts were recently revealed by Theopold.⁸

Results and discussion

Synthesis and characterization of hydroxochromium(II) complexes

Hydroxometal complexes ($\text{M}-\text{OH}$) are versatile precursors for coordination complexes, because acidic substrates ($\text{H}-\text{A}$)

undergo dehydrative condensation to give products coordinated by the conjugated base of the acidic substrate ($\text{M}-\text{OH} + \text{H}-\text{A} \rightarrow \text{M}-\text{A} + \text{H}_2\text{O}$).⁹ Typical synthetic methods for hydroxo complexes involve basic hydrolysis of the corresponding halide. Treatment of the dinuclear μ -chlorochromium(II) complex **1**⁶ with aqueous NaOH solution in THF or methanol gave the hydroxo complex **3** as blue crystals after evaporation and extraction with ether followed by crystallization from pentane (Scheme 1). Because all Cr(II) species described in this paper were very sensitive to the air, preparation of the Cr(II) complexes was carried out in a glove box filled with argon. The hydroxo complex **3** was also obtained from the pyridine adduct **2a** upon treatment with aqueous NaOH solution. It is essential to use *aqueous* NaOH solution. Otherwise, for example, reaction of **2a** with methanolic NaOH solution in MeOH gave the trinuclear μ -methoxo complex, $\text{Tp}^{\text{iPr}_2}\text{Cr}(\mu\text{-OMe})_2\text{Cr}(\mu\text{-OMe})_2\text{CrTp}^{\text{iPr}_2}$,¹⁰ the central chromium atom in which should come from partial decomposition of the $\text{Tp}^{\text{iPr}_2}\text{Cr}$ fragment.



The analogous reaction of the pyrazole adduct **2b**, however, caused concomitant deprotonation to give the dinuclear μ -hydroxo- μ -pyrazolato complex **4** (Scheme 1). Similar complexes of other first row metals [$(\mu\text{-OH})(\mu\text{-pz}^{\text{R}})(\text{MTp}^{\text{R}})_2$]¹¹ were obtained upon hydrolysis of $(\mu\text{-Cl})_2(\text{MTp}^{\text{R}})_2$ (in particular, for complexes bearing a less hindered ligand such as Tp^{Me_2} and its 4-substituted derivatives), where the bridging pyrazolato ligand should be formed by partial hydrolysis of the Tp^{R} ligand.

† Electronic supplementary information (ESI) available: Atomic numbering schemes. See <http://www.rsc.org/suppdata/dt/b3/b309762e/>

‡ Present address: Department of Applied Chemistry, School of Engineering, University of Tokyo, Hongo, Bunkyo-ku, Tokyo 113-8656, Japan.

IR spectra for the hydroxochromium complexes contain ν_{OH} vibrations at 3718 (**3**) and 3685 cm^{-1} (**4**), suggesting hydrolysis of the Cr–Cl functional group in **1** and **2**, and the paramagnetic products are characterized by X-ray crystallography. Molecular structures of **3** and **4** are shown in Fig. 1 and 2, and selected structural parameters are summarized in Table 1. The dinuclear μ -hydroxo complex **3** sitting on a centrosymmetric site is found to be isostructural with the starting complex **1** with the virtually square-pyramidal coordination geometry. The square-pyramidal geometry is evident from the τ value¹² being very close to 0 and the Cr–N(axial) distances are substantially longer than the Cr–N(equatorial) distances, as was also observed for the chloro complex **1**. The Cr–O separations⁸ fall in the range of single bond lengths (~ 1.8 Å) and is much longer than the Cr=O lengths (~ 1.6 Å) as well. The μ -pyrazolato complex **4** is virtually of C_2 symmetry with respect to the axis passing through O1 and the midpoint of the N71–N72 bond. Replacement of one of the two hydroxo ligands in **3** by the rather bulky pyrazolato bridge causes distortion of the square-pyramidal geometry as is indicated by the τ values (~ 0.3), which are substantially larger than those for **1** (0.06) but still small (< 0.5) indicating the square-pyramidal geometry. The Cr–N and Cr–O lengths for **3** and **4** are comparable.

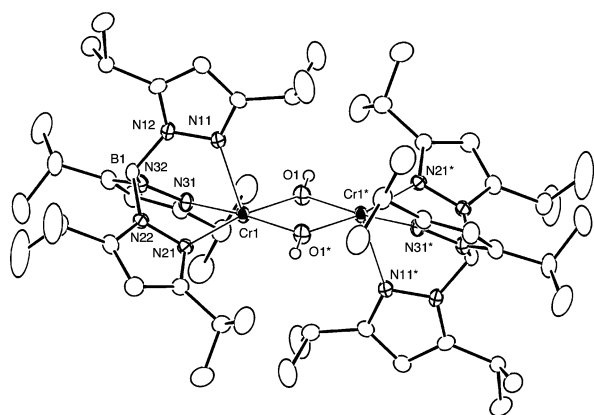


Fig. 1 Molecular structures of **3** (one of two independent molecules: A series) showing the 30% thermal ellipsoids.

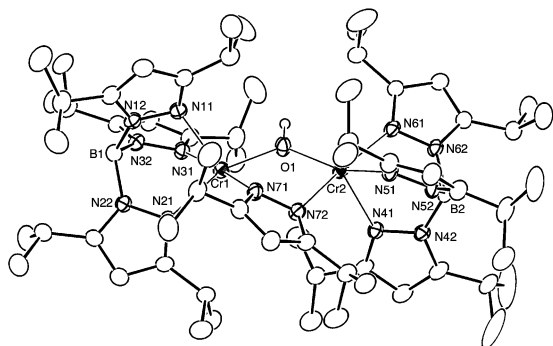


Fig. 2 Molecular structure of **4**. Thermal ellipsoids are drawn at the 30% probability level.

The basic property of the hydroxo complex **1** was also confirmed by dehydrative condensation with acetic acid to give the μ -hydroxo- μ -acetato complex, $\text{Tp}^{\text{IPr}_2}\text{Cr}(\mu\text{-OH})(\mu\text{-OAc})\text{-CrTp}^{\text{IPr}_2}$.¹³

Oxidative addition reactions to hydroxochromium(II) complex **3**. (a) Reaction with organic chloride

In the previous paper we reported that chlorochromium(II) complexes including **1** and **2** are readily susceptible to one-electron oxidative addition of organic halide to give chromium(III) species.⁶ As a preliminary study, the hydroxo complex **3**

was subjected to reaction with the organic chlorides, which were previously used for the reactivity study of the chloro complexes **1** and **2**. Addition of two equivalents (molar ratio) of benzyl chloride or methylene chloride to **3** gave the air-stable, red product **5**, which was isolated by crystallization from THF–MeCN (Scheme 2). An IR spectrum of **5** contains a ν_{OH} band (3643 cm^{-1}) together with two B–H vibrations (2551, 2471 cm^{-1}) suggesting the presence of two Tp^{IPr_2} ligands with different coordination modes. In a previous paper we reported that the B–H band was a good indicator for the coordination mode of Tp^{R} ligands, *i.e.*, in the case of Tp^{IPr_2} complexes, the B–H vibration of a κ^3 - and κ^2 -coordinated Tp^{IPr_2} ligand appear above and below 2500 cm^{-1} , respectively.¹⁴ The ν_{BH} values observed for **5** fell in the range typical for those for a κ^3 - and κ^2 - Tp^{IPr_2} ligand, respectively. The parent peak observed by an FD-MS measurement [m/z (M^+) = 1121] was consistent with the formulation of $(\text{Tp}^{\text{IPr}_2}\text{Cr})_2(\text{OH})_3(\text{Cl})$ and the molecular structure of **5** was confirmed by X-ray crystallography (Fig. 3 and Table 1).

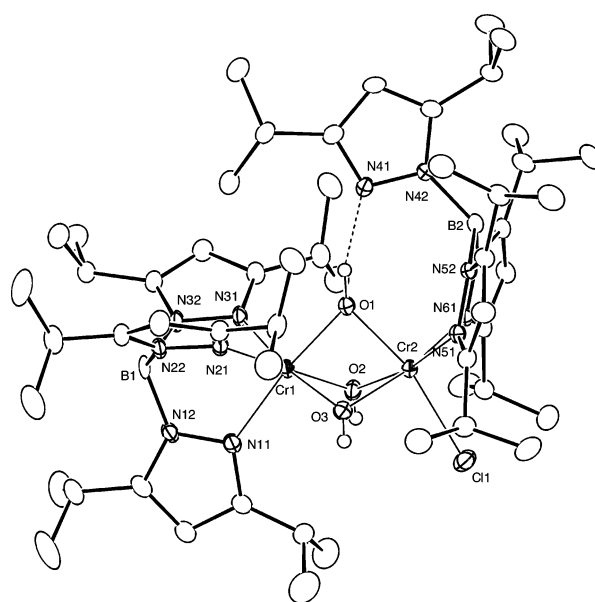
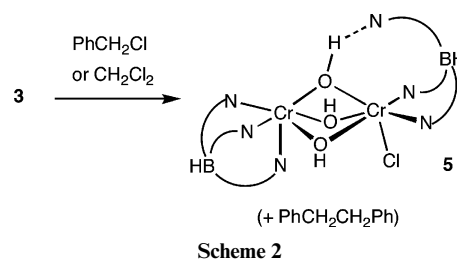


Fig. 3 Molecular structure of **5**. Thermal ellipsoids are drawn at the 30% probability level.

The red product **5** has been characterized as the dinuclear tri(μ -hydroxo)chloro complex of chromium(III) resulting from one-electron oxidative addition of organic halide. In accord with the IR result (ν_{BH}) the complex contains two Tp^{IPr_2} ligands of the different coordination geometries. One of the two chromium centers (Cr1) is coordinated by the κ^3 - Tp^{IPr_2} ligand and the three bridging hydroxo ligands to form the octahedral coordination geometry, whereas the other chromium center (Cr2) adopts the octahedral geometry coordinated by the κ^2 - Tp^{IPr_2} ligand in addition to the terminal chloro and the three bridging hydroxo ligands. In contrast to the square-pyramidal geometry observed for the Cr(II) species (*e.g.* **1–4**), the Cr(III) centers in **5** adopt octahedral coordination geometry. It is notable that the non-coordinated pyrazolyl nitrogen atom (N41) is located at the distance of hydrogen-bonding interaction with one of the

Table 1 Selected structural parameters for Tp^{IPr}Cr–OH complexes

Complexes	3 (mol1)	3 (mol2)	4 (Cr1)	(Cr2)	5 (Cr1)	(Cr2) ^a
X	O1	O2	O1	O1	O1	O1
Y	O1*	O2*	N71	N72	O2	O2
Z	—	—	—	—	O3	O3
Bond lengths/Å						
Cr–N11(41)	2.360(3)	2.412(5)	2.353(3)	2.364(3)	2.071(3)	—
Cr–N21(51)	2.142(5)	2.153(4)	2.162(4)	2.106(4)	2.072(3)	2.041(3)
Cr–N31(61)	2.142(4)	2.124(4)	2.162(4)	2.165(3)	2.059(3)	2.053(3)
Cr–X	2.021(4)	2.033(4)	2.029(3)	2.038(4)	1.923(3)	1.936(2)
Cr–Y	2.022(3)	1.979(3)	2.083(4)	2.097(3)	1.975(2)	2.004(2)
Cr–Z	—	—	—	—	1.985(2)	2.008(3)
Bond angles/°						
N11(41)–Cr–N21(51)	83.9(1)	81.7(2)	92.3(1)	91.9(1)	87.3(1)	—
N11(41)–Cr–N31(61)	88.1(1)	88.2(2)	80.5(1)	83.9(1)	88.7(1)	—
N11(41)–Cr–X	104.4(1)	106.1(2)	110.2(1)	114.0(1)	172.3(1)	—
N11(41)–Cr–Y	101.4(1)	105.2(2)	98.9(1)	95.7(1)	94.0(1)	—
N11(41)–Cr–Z	—	—	—	—	99.0(1)	—
N21(51)–Cr–N31(61)	85.4(2)	86.6(1)	98.9(1)	81.0(1)	88.5(1)	87.0(1)
N21(51)–Cr–X	170.9(1)	172.0(2)	157.5(1)	154.1(1)	99.6(1)	91.91(9)
N21(51)–Cr–Y	99.3(2)	100.2(1)	91.4(1)	91.1(1)	177.8(1)	169.92(9)
N21(51)–Cr–Z	—	—	—	—	95.8(1)	97.5(1)
N31(61)–Cr–X	98.4(2)	95.2(2)	99.6(1)	102.1(1)	99.0(1)	95.0(1)
N31(61)–Cr–Y	169.8(1)	165.7(2)	175.8(1)	172.1(1)	95.8(1)	93.1(1)
N31(61)–Cr–Z	—	—	—	—	171.4(1)	170.17(9)
X–Cr–Y	75.7(2)	76.4(1)	84.5(1)	85.3(1)	79.0(1)	78.04(9)
X–Cr–Z	—	—	—	—	76.9(1)	76.1(1)
Y–Cr–Z	—	—	—	—	82.2(1)	81.0(1)
Cr–O–Cr	104.3(2)	103.6(1)	121.0(2)	—	87.9(1), ^c 84.63(9), ^d 84.2(1) ^e	—
τ^f	0.018	0.105	0.305	0.300	—	—
Complexes						
	10	11 (Cr1)	(Cr2) ^b			
X	O1	O1	O1			
Y	O2	O2	O2			
Z	O3	O3	O3			
Bond lengths/Å						
Cr–N11(41)	2.065(2)	2.067(3)	2.665(4)			
Cr–N21(51)	2.099(2)	2.074(3)	2.063(3)			
Cr–N31(61)	2.103(2)	2.093(3)	2.040(3)			
Cr–X	2.005(2)	1.921(2)	1.960(3)			
Cr–Y	1.939(2)	1.984(2)	2.027(2)			
Cr–Z	1.927(2)	1.968(3)	1.999(2)			
Bond angles/°						
N11(41)–Cr–N21(51)	87.01(8)	87.2(1)	—			
N11(41)–Cr–N31(61)	87.61(7)	87.0(1)	—			
N11(41)–Cr–X	177.74(7)	173.6(1)	—			
N11(41)–Cr–Y	92.51(8)	92.7(1)	—			
N11(41)–Cr–Z	92.54(7)	100.9(1)	—			
N21(51)–Cr–N31(61)	86.48(7)	89.6(1)	86.6(1)			
N21(51)–Cr–X	91.34(7)	99.2(1)	91.4(1)			
N21(51)–Cr–Y	177.25(7)	174.8(1)	169.9(1)			
N21(51)–Cr–Z	91.53(7)	94.5(1)	102.2(1)			
N31(61)–Cr–X	90.76(7)	92.7(1)	96.6(1)			
N31(61)–Cr–Y	90.80(6)	95.6(1)	91.7(1)			
N31(61)–Cr–Z	178.00(7)	171.2(1)	169.3(1)			
X–Cr–Y	89.07(7)	80.91(9)	78.93(9)			
X–Cr–Z	89.05(7)	79.0(1)	77.4(1)			
Y–Cr–Z	91.19(7)	80.3(1)	78.53(9)			
Cr–O–Cr	—	87.2(1), ^c 83.70(8), ^d 84.8(1) ^e	—			
τ^f	—	—	—			

^a Cr2–Cl1: 2.3302(9) Å. ^b Cr2–O4: 1.933(3) Å. ^c Cr1–O1–Cr2. ^d Cr1–O2–Cr2. ^e Cr1–O3–Cr2. ^f Ref. 12.

three bridging hydroxo ligands (O1: 2.672(4) Å). Such an interaction is also supported by the orientation of the lone pair electrons of N41, which are directed toward O1. Compared to an alternative isomeric structure with one terminal hydroxo ligand and two κ^3 -Tp^{IPr} ligands, (κ^3 -Tp^{IPr})Cr(OH)(μ -OH)₂-Cr(κ^3 -Tp^{IPr})(Cl), the actual form may be able to release steric repulsion between the two bulky Tp^{IPr} ligands. In accord with

this consideration, the Cr–O1 distances are substantially shorter than the Cr–O_{2,3} distances.

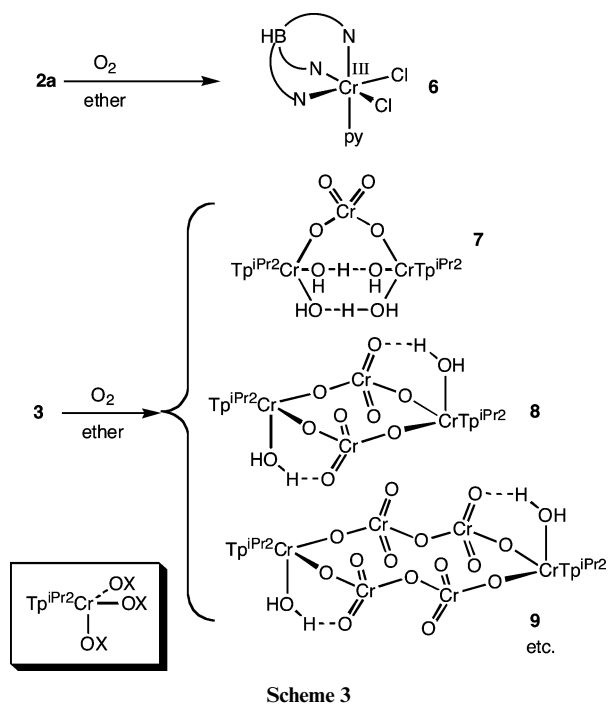
The chloro ligand in **5** should result from oxidative addition, which is supported by detection of diphenylethane by GC-MS analysis of a reaction mixture obtained from benzyl chloride. Although the direct oxidative addition product should be [Tp^{IPr}Cr(OH)(Cl)]_n (*n* = 1, 2), the tri(μ -hydroxo) complex **5** may

be formed by coupling of the monomeric intermediate, $\text{Tp}^{\text{IPr}_2}\text{Cr}(\text{OH})(\text{Cl})$, with **3** followed by further one-electron oxidation and addition of the OH fragment coming from adventitious water in the reaction mixture.

(b) Attempted O_2 -oxidative addition to chromium(II) complexes

The results obtained so far suggested that a peroxo species might be obtained by O_2 -oxidative addition to low valent chromium(II) species **2a** and **3**. In the case of the vanadium and manganese systems the hydroxo complexes were converted to peroxo species *via* O_2 -oxidative addition: $\text{Tp}^{\text{IPr}_2}\text{V}(\text{O})(\text{OH})(\text{OH}_2) + \text{O}_2 \rightarrow \text{Tp}^{\text{IPr}_2}\text{V}(=\text{O})(\text{O}_2)(\text{H}-\text{pz}^{\text{IPr}_2})$; $(\mu\text{-OH})_2(\text{MnTp}^{\text{IPr}_2})_2 + \text{O}_2 \rightarrow "(\mu\text{-O}_2)(\mu\text{-OH})_2(\text{MnTp}^{\text{IPr}_2})_2" \rightarrow (\mu\text{-O})(\text{MnTp}^{\text{IPr}_2})_2$.¹⁵ Very recently Theopold reported formation of a new type of a Cr– O_2 adduct, a superoxochromium(III) species $[\text{Tp}^{\text{tBu,Me}}\text{Cr}^{\text{III}}(\text{O}_2^-)(\text{pz}^{\text{tBu,Me}}\text{-H})]^+\text{BARF}^-$, by O_2 -oxidative addition to a coordinatively unsaturated Cr(II) species, $[\text{Tp}^{\text{tBu,Me}}\text{Cr}^{\text{II}}(\text{pz}^{\text{tBu,Me}}\text{-H})]^+\text{BARF}^-$.⁸

Exposure of an ethereal solution of the chlorochromium(II) complex **2a** to O_2 (1 atm) at -78°C caused immediate color change from green to pink and, upon warming to room temperature, further color change into brown was observed (Scheme 3). The resultant residue was characterized as the dichlorochromium(III) complex **6** by comparison of its IR spectrum with an authentic sample of **6**, which was obtained by treatment of **2a** with benzyl chloride as reported in the previous paper.⁶ Although the pink intermediate formed at the low temperature could be a peroxo intermediate, $\text{Tp}^{\text{IPr}_2}\text{Cr}(\text{O}_2)(\text{py})(\text{Cl})$ or $(\mu\text{-O}_2)[\text{CrTp}^{\text{IPr}_2}\text{Cl}]_2$,¹⁶ further characterization could not be made due to its thermal instability.



O_2 -treatment of the hydroxochromium(II) complex **3** also resulted in immediate color change from blue to brown to give a low yield mixture, from which several types of single crystals were obtained by crystallization from pentane (Scheme 3). X-ray crystallography of single crystals **7–9**¹⁷ separated by hand revealed that they were dinuclear complexes with the bridging chromato or dichromato ligand(s) as shown in Scheme 3.¹⁸ The aquo ligands are in the range of separations for hydrogen bonds from the neighboring oxygen-functional groups [2.470(3), 2.474(3) Å (**7**: from CrOH); 2.820(7) Å (**9**: from Cr=O)]. Because they can not be prepared in a selective manner despite many attempts and are characterized only by crystallo-

graphy, details will not be discussed here and the crystallographic results are included in the ESI.† But it should be noted that no evidence for formation of peroxo complex could be detected. The O_2 -treatment causes (1) oxidation of the $\text{Tp}^{\text{IPr}_2}\text{Cr}(\text{II})$ centers to Cr(III) as observed for the chloro complex **2** and (2) formation of the chromate and dichromate bridges containing the Cr(VI) centers *via* partial oxidative degradation of the $\text{Tp}^{\text{IPr}_2}\text{Cr}$ fragment. The obtained results are in sharp contrast to the results reported for the $\text{Tp}^{\text{tBu,Me}}$ system (see above).⁸ We also attempted oxygenation of **2** under the conditions similar to those for the $\text{Tp}^{\text{tBu,Me}}$ system but could not get any evidence for formation of an O_2 -adduct. The difference should be ascribed to the steric effect of the Tp^{R} ligands as typically observed for $[\text{Tp}^{\text{R}}\text{CrCl}]_n$.⁶ The Tp^{IPr_2} complex forms the dinuclear, square-pyramidal species with the two μ -chloro ligands ($n = 2$), whereas the $\text{Tp}^{\text{tBu,Me}}$ derivative gives the four-coordinate species ($n = 1$) with so-called *cis*-divacant structure,⁸ which may be essential for the O_2 -coordination. No such a coordination structure has been observed for the Tp^{IPr_2} system.

Apart from the peroxo chemistry, in the structures of **7–9** (and **5**) the $\text{Tp}^{\text{IPr}_2}\text{Cr}(\text{III})$ moiety serves as a corner block (Scheme 3), which connects three oxygen ligands with the angles close to the right angle in a *cis*-fashion. Such behavior is frequently observed for $\text{Tp}^{\text{R}}\text{M}$ complexes¹⁸ and may be utilized as a component of supramolecules. Various O-ligands including OH_x and ester residues (carboxylate, CrO_4^- , $\text{Cr}_2\text{O}_7^{2-}$) could be used as components to be linked.

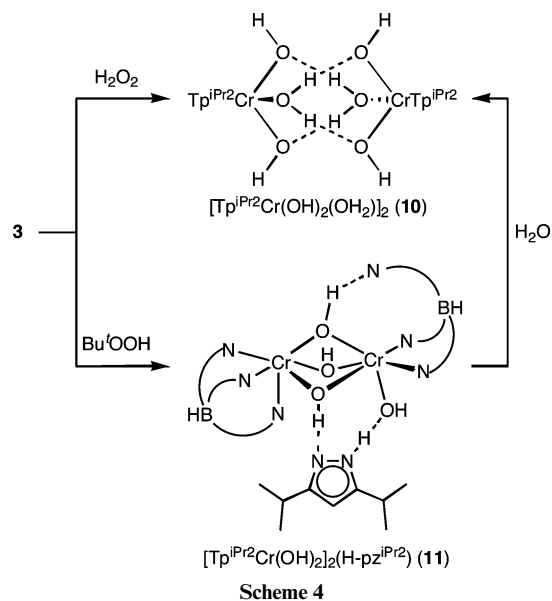
Thus O_2 -oxidative addition to the low valent $\text{Tp}^{\text{IPr}_2}\text{Cr}(\text{II})$ complexes **2a** and **3** resulted in one-electron oxidation of the chromium center to give the $\text{Tp}^{\text{IPr}_2}\text{Cr}(\text{III})$ complexes **6–9**.

Synthesis of hydroxochromium(III) complex **3**.

(a) Attempted dehydrative condensation with ROOH

Dehydrative condensation of a hydroxo complex with H_2O_2 is a useful synthetic method for a peroxo complex developed in our laboratory and a variety of $\text{Tp}^{\text{R}}\text{M}-\text{O}_2$ adducts have been prepared by this method.² Analogous condensation with alkyl hydroperoxide produced the corresponding alkylperoxo complexes, which are also regarded as key intermediates of oxygenation reactions. Then the hydroxochromium(II) complex **3** was subjected to reaction with H_2O_2 and *t*-BuOOH in hope of formation of Cr(II)-peroxo species, $(\mu\text{-O}_2)(\text{CrTp}^{\text{IPr}_2})_2$ and $\text{Tp}^{\text{IPr}_2}\text{Cr}-\text{OOR}$.

Addition of an aqueous H_2O_2 solution to an ethereal solution of **3** at -78°C gave a brown solution, when the mixture was gradually warmed to 0°C . Concentration followed by cooling at -30°C gave the red-brown product **10** (Scheme 4),



which showed IR bands associated with aquo and hydroxo ligands ($3670, 1645\text{ cm}^{-1}$). Complex **10** was characterized as a dimeric di(hydroxo)(aquo)chromium(III) complex as determined by X-ray crystallography (see below). The original product should be a five-coordinate $\text{Tp}^{\text{iPr}_2}\text{Cr}(\text{OH})_2$ complex but the Cr(III) center takes up one water molecule to attain the octahedral geometry, the coordination geometry which Cr(III) species prefer. Thus reaction of **3** with H_2O_2 also resulted in one-electron oxidation to give the trivalent dihydroxo complex **10**, which would be susceptible to further dehydrative condensation (see below).

Reaction with *t*-BuOOH also caused one-electron oxidation of the Cr center to give the brown product **11** $[\text{Tp}^{\text{iPr}_2}\text{Cr}(\text{OH})_2]_2 \cdot (\text{H-pz}^{\text{iPr}_2})$, which was found to be a pyrazole-adduct of a formally dehydrated form of **10**, $[\text{Tp}^{\text{iPr}_2}\text{Cr}(\text{OH})_2]_2$, as determined by X-ray crystallography (see below). An IR spectrum of **11** showed the feature (two ν_{BH}) similar to that of the chloro complex **5** discussed above. In accord with the dehydrated structure, the bending band of the aquo ligand observed for **10** (1645 cm^{-1}) disappeared but the ν_{OH} band for the hydroxo ligand remained. The pyrazole-adduct **11** was converted to the hydrated form **10** upon treatment with water.

Molecular structures of **10** and **11** determined by X-ray crystallography are shown in Fig. 4 and 5, respectively, and selected structural parameters are summarized in Table 1. As for the hydrated form **10**, coordination of the $\kappa^3\text{-Tp}^{\text{iPr}_2}$ ligand and three OH_x ligands to the Cr(III) center leads to the octahedral coordination geometry and further hydrogen bonding interactions among the OH_x ligands leads to the dimeric structure. Judging from the $\text{O} \cdots \text{O}$ separations, the $\text{O1} \cdots \text{O2}^*$ and $\text{O1} \cdots \text{O3}^*$ pairs are connected by hydrogen bonding interactions [$\text{O1} \cdots \text{O2}^*$: $2.553(2)$; $\text{O1} \cdots \text{O3}^*$: $2.616(2)\text{ \AA}$; others $> 3.0\text{ \AA}$]. The mononuclear unit contains four protons, of which two should be involved in the hydrogen bonds. The remaining two protons therefore should be attached to the O2 and O3 atoms. These structural features lead to the assignments of the O1 atom as the aquo ligand, the O2 and O3 atoms as the hydroxo ligands and, as a whole, complex **10** as the dimeric (aquo)(dihydroxo)chromium(III) complex. Accordingly, the Cr1–O1(aquo) distance is slightly longer than the Cr1–O2,3-(hydroxo) distances (the differences $> 0.06\text{ \AA}$). $\text{Tp}^{\text{R}}\text{M}(\text{OH})_3$ fragments frequently form this type of hydrogen bonding

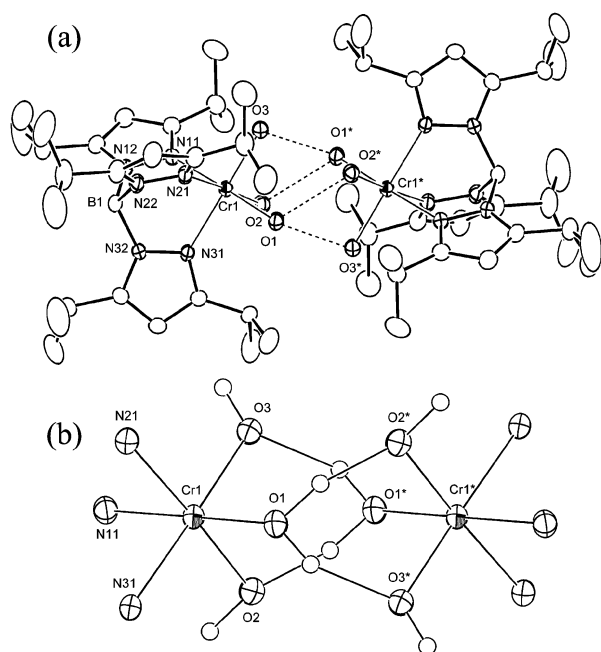


Fig. 4 Molecular structure of **10**. Thermal ellipsoids are drawn at the 30% probability level. (a) An overview. (b) An expanded view of the core part.

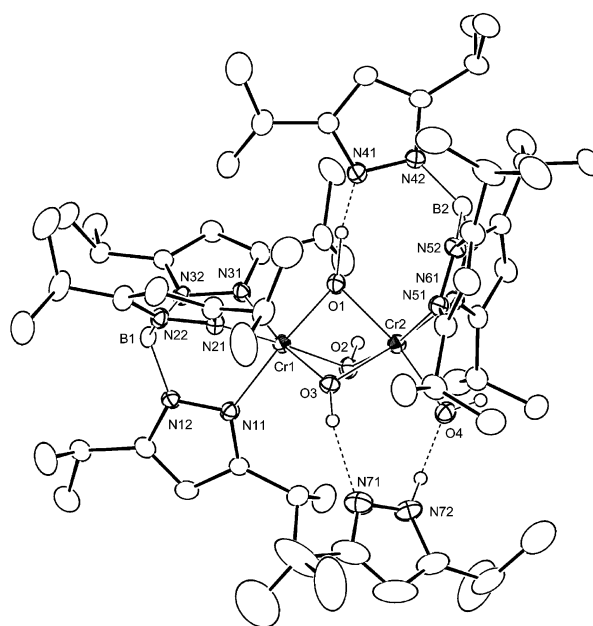
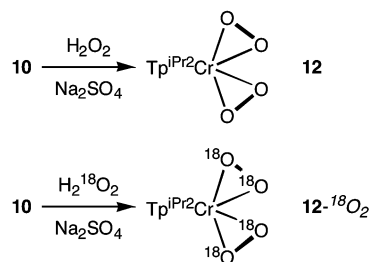


Fig. 5 Molecular structure of **11**. Thermal ellipsoids are drawn at the 30% probability level.

networks to form a dimeric structure as we recently reported for the ruthenium system.¹⁹ The dehydrated form **11** is characterized as an adduct of the pyrazole molecule ($\text{H-pz}^{\text{iPr}_2}$), which should be formed by partial decomposition of the Tp^{iPr_2} ligand.¹¹ Structural features of the core part are essentially the same as those of the chloro derivative **5**, *i.e.* (1) the two chromium centers are bridged by the three hydroxo ligands (O1–3), (2) the Tp^{iPr_2} ligands are coordinated to the chromium centers in $\kappa^3(\text{Cr1})$ - and $\kappa^2(\text{Cr2})$ -fashions, and (3) one of them forms a hydrogen-bonding interaction with the non-coordinated pyrazolyl nitrogen atom [$\text{Cr2} \cdots \text{N41}$: $4.070(4)\text{ \AA}$; $\text{O1} \cdots \text{N41}$: $2.646(4)\text{ \AA}$]. The Cr–O1 distances are substantially shorter than the Cr1–O2 and Cr1–O3 distances as observed for **5** and the Cr–O distance for the terminal hydroxo ligand (Cr2–O4) is comparable to the short Cr–O1 distances. Replacement of the chloro ligand in **5** by the hydroxo ligand (O4) provides an opportunity to form hydrogen bonding interaction with a protic substrate, the pyrazole auxiliary. The $\text{O4} \cdots \text{N72}$ [$2.642(5)\text{ \AA}$] and $\text{O3} \cdots \text{N71}$ [$2.974(5)\text{ \AA}$] separations are in the range for the distances of hydrogen-bonding interactions.

Diperoxo-chromium(v) complex **12**. (a) Synthesis and characterization

The dihydroxo-chromium(III) complex **10** obtained by oxidation of the hydroxo-chromium(II) complex **3** contained Cr–OH functional groups, which might undergo dehydrative condensation with H_2O_2 leading to a peroxo species. Treatment of **10** with H_2O_2 at $-78\text{ }^\circ\text{C}$ in the presence of a dehydrating agent (Na_2SO_4) resulted in a color change from blue to red–brown and from the resultant mixture the green product **12** was isolated after extraction with pentane followed by crystallization (Scheme 5). Complex **12** was rather thermally unstable and



Scheme 5

gradually decomposed when left at room temperature. The rather intense IR absorptions observed for **12** at 945 and 888 cm^{-1} (Fig. 6a) fall in the range of O–O vibrations of peroxometal complexes.¹ Although such vibrations are, in principle, IR-inactive, the product **10** is assigned as a diperoxo complex on the basis of the results of the labeling experiments.

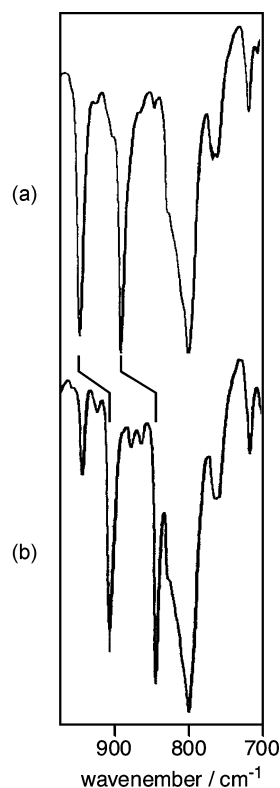


Fig. 6 IR spectra ($\nu_{\text{O-O}}$ region; KBr pellet) of (a) **12** and (b) **12**- $^{18}\text{O}_2$.

In order to confirm the tentatively assigned O–O vibrations (945, 888 cm^{-1}) an $^{18}\text{O}_2$ -labeled sample was prepared by treatment of **10** with $\text{H}_2^{18}\text{O}_2$ (Scheme 4) and its IR spectrum is shown in Fig. 6b. The shift of both of the two vibrations to lower energies (904, 841 cm^{-1}) clearly indicated that the absorptions were associated with an ^{18}O atom. The extent of the shifts to lower energies [for the vibration at 945 cm^{-1} : $\Delta\nu = 41 \text{ cm}^{-1}$, $\nu(^{18}\text{O}-^{18}\text{O})/\nu(^{16}\text{O}-^{16}\text{O}) = 0.967$; for the vibration at 888 cm^{-1} : $\Delta\nu = 47 \text{ cm}^{-1}$, $\nu(^{18}\text{O}-^{18}\text{O})/\nu(^{16}\text{O}-^{16}\text{O}) = 0.947$] are found to be very close to the calculated values based on the isotopic shift [$\nu(^{18}\text{O}-^{18}\text{O})/\nu(^{16}\text{O}-^{16}\text{O}) = 0.943$]. An FD-MS spectrum of **12**, however, did not contain the expected parent peak [$m/z = 582 (\text{M}^+)$] but the peaks at $m/z = 566 (\text{M}^+ - \text{O})$, 550 ($\text{M}^+ - 2\text{O}$), 536 ($\text{M}^+ - 3\text{O}$) corresponding to the deoxygenated forms. This result raised a problem about the proposed structure of **12**. Because

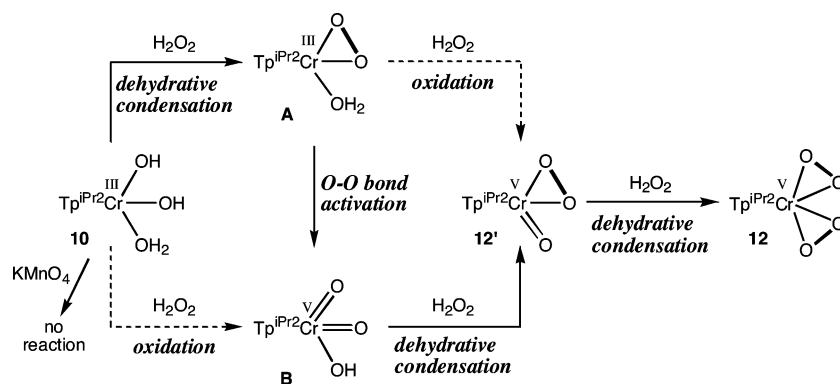
$\nu_{\text{Cr=O}}$ vibrations appear around 900 cm^{-1} ⁸ and the calculated isotopic shift (0.957) was virtually the same as that for the O–O vibration within the experimental error, the result of the labeling experiment was not enough to eliminate the structures containing an oxo ligand, $\text{Tp}^{\text{iPr}_2}\text{Cr}(\text{O}_2)(=\text{O})$ **12'** and $\text{Tp}^{\text{iPr}_2}\text{Cr}(=\text{O})_2$ **12''**. Although we tried Raman measurements to discriminate an O–O vibration from a Cr=O vibration, no definite conclusion was obtained due to the thermal instability of **12**. Then we tried to characterize **12** by chemical processes (Scheme 6). Both of the $\text{M}(\text{O}_2)$ and $\text{M}=\text{O}$ functional groups are known to be labile with respect to hydrolytic cleavage. Treatment of **12** (**12'**, **12''**) with $\text{H}_2^{18}\text{O}_2$, therefore, is expected to result in replacement of the $\text{Cr}(\text{O}_2)$ moiety by the $^{18}\text{O}_2$ isotope, whereas that with H_2^{18}O is expected to cause ^{18}O -labeling of the $\text{Cr}(=\text{O})$ moiety. Actually, treatment with $\text{H}_2^{18}\text{O}_2$ caused appearance of IR bands identical to those of **12**- $^{18}\text{O}_2$ (Fig. 6b) and no change was observed upon treatment with H_2^{18}O . These results clearly indicate that the obtained product is the diperoxo species **12**.²⁰

($\text{O}^*: ^{18}\text{O}$)

H_2^{18}O treatment	possible structures	$\text{H}_2^{18}\text{O}_2$ treatment
no change		shifts of of the two bands

Scheme 6

The conversion of the dihydroxochromium(III) complex **10** into the diperoxochromium(V) complex **12** involves concomitant dehydrative condensation with H_2O_2 and oxidation of the metal center, in other words, oxidative dehydrative condensation. Plausible formation mechanisms for **12** are summarized in Scheme 7. Although the final process should be dehydrative condensation of the $\text{Cr}=\text{O}$ group in **12'** with H_2O_2 to give **12**,⁵ the intermediate **12'** could be formed *via* the processes shown in Scheme 7. We tried to detect the intermediates by the reaction with a limited amount of H_2O_2 but merely a mixture of the unreacted **10** and the oxidized product **12** was obtained. In order to examine the oxidation process of the $\text{Cr}-\text{OH}$ group in

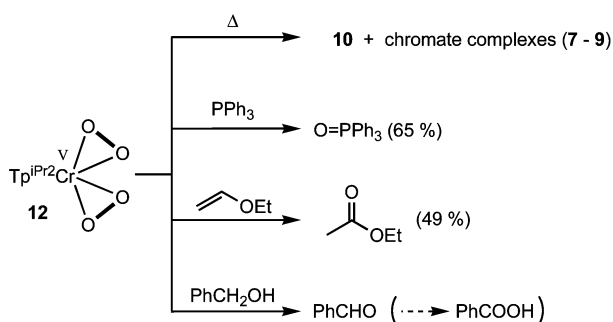


Scheme 7

10 leading to the Cr=O functional group complex **10** was treated with oxidizing agents such as KMnO_4 but the hydroxo complex **10** was recovered unaffected, indicating that the oxidative Cr–OH \rightarrow Cr=O conversion was not a viable process. On the basis of this result we propose the processes shown in Scheme 7. Initial dehydrative condensation of the dihydroxo complex **10** with H_2O_2 should give the monoperoxo intermediate **A**, the oxidative O–O bond cleavage process of which should give the dioxochromium(v) intermediate **B**. Double dehydrative condensation of the oxo groups with H_2O_2 finally produces the diperoxo species **12**.

(b) Oxidation reactions with the diperoxochromium(v) species **12**

The oxidizing ability of the resultant diperoxo species **12** was examined. Although the diperoxo complex **12** was definitely stable when kept at -78°C , slow decomposition was observed when left at room temperature (Scheme 8). The resultant complicated mixture contained the dihydroxo complex **10** and the chromate complexes **7–9** as judged by an IR spectrum of the mixture. The formation of the Cr(III) species **10** under the inert atmosphere suggested that the decomposition process involved a thermally induced disproportionation process.



Scheme 8

Oxygenation ability of **12** was evidenced by the reaction with PPh_3 , which gave O=PPh_3 in 65% yield. (The yield is based on the two peroxo ligands in **12**. In the case of quantitative formation of O=PPh_3 , two moles of O=PPh_3 are formed from one mole of **12**.) Addition of PPh_3 immediately caused color change from green to brown to give a mixture of chromium complexes (**7–10**) similar to that obtained from spontaneous thermal decomposition of **12**. The oxo transfer reaction should leave oxo species like **12'** and **B**, decomposition of which might give a mixture of the chromium complexes. It is notable that the peroxochromium species **12** showed a remarkable oxidation ability, when compared with the related $\text{Tp}^{\text{R}}\text{M}(\text{O}_2)$ species of early transition metals [$\text{Tp}^{\text{iPr}_2}\text{V}^{\text{V}}(\text{O}_2)(=\text{O})(\text{pz}^{\text{iPr}_2}\text{-H})$;⁵ $\text{Tp}^{\text{iPr}_2}\text{Mn}^{\text{III}}(\text{O}_2)(\text{pz}^{\text{iPr}_2}\text{-H})$]¹⁵]; oxygenation of PPh_3 by such species was very sluggish. Olefin oxygenation was examined with vinyl ether and styrene. The reaction with ethyl vinyl ether produced ethyl acetate in 49% yield as determined by GLC analysis, while no oxidized product was detected for styrene by GLC analysis of the reaction mixture. The effective oxygenation of the electron-rich vinyl ether confirms electrophilic nature of **12**. Finally, benzyl alcohol was converted to benzaldehyde, which was further converted to benzoic acid.

Conclusions

Synthesis of a peroxochromium complex is examined by dehydrative condensation of a hydroxo complex with H_2O_2 and O_2 -oxidative addition. The dimeric hydroxochromium(II) complex, $(\mu\text{-OH})_2(\text{CrTp}^{\text{iPr}_2})_2$ **3**, is obtained by hydrolysis of the corresponding chloride **1**. Reaction of **3** with oxygenating agents (O_2 , H_2O_2 , and ROOH) and chloroalkanes results in one-electron oxidation of the metal center to give to a variety of hydroxo-

chromium(III) complexes including the κ^1 -dihydroxo complex, $[\text{Tp}^{\text{iPr}_2}\text{Cr}(\text{OH})_2(\text{OH}_2)]_2$ (**10**), and μ -hydroxo complexes, $(\kappa^3\text{-Tp}^{\text{iPr}_2})\text{Cr}(\mu\text{-OH})_3\text{Cr}(\kappa^2\text{-Tp}^{\text{iPr}_2})(\text{X})$ [$\text{X} = \text{Cl}$ (**5**), OH (**11**)]. Further treatment of **10** with H_2O_2 produces the diperoxo complex, $\text{Tp}^{\text{iPr}_2}\text{Cr}^{\text{V}}(\text{O}_2)_2$ **12**, via oxidative dehydrative condensation and complex **12** has been characterized by the spectroscopic methods and the labeling experiments. The diperoxochromium(v) species **12** exhibits moderate oxygenation activity based on its electrophilic nature and the oxidizing ability is remarkably higher than that of the related $\text{Tp}^{\text{R}}\text{M}-\text{O}_2$ adducts of early transition metals (V, Mn), which are sluggish even toward PPh_3 (a readily oxidizable substrate), indicating that the oxidation ability of peroxo species coordinated by the Tp^{iPr_2} ligand is highly dependent on the kind of the central metal and its oxidation state.

Experimental

Preparation of **3** and **4** was carried out in a glove box filled with argon and other experiments were carried out under an argon atmosphere using standard Schlenk tube technique. CH_2Cl_2 (P_4O_{10}), MeOH ($\text{Mg}(\text{OMe})_2$), MeCN (CaH_2), THF, pentane and hexane (Na–K/benzophenone) were treated with appropriate drying agents, distilled, and stored under argon. IR (measured as KBr pellets; reported in cm^{-1}) and FD-MS spectra were obtained on a JASCO FT/IR 5300 and JEOL JMS-700 spectrometer, respectively. ^{31}P -NMR spectra were obtained on a Bruker AC-200 spectrometer. Starting complexes **1** and **2a,b** were prepared according to the procedures reported in our previous paper.⁶ Other chemicals were used as received without further purification.

Preparation of $[\text{Tp}^{\text{iPr}_2}\text{Cr}(\text{OH})_2]$ **3**

Upon addition of an aqueous NaOH solution (1.5 M, 5 mL) to a THF solution (10 mL) of the chloro complex **1** (103 mg, 0.093 mmol) the color of the mixture changed from green to blue. Then the volatiles were removed under reduced pressure and the residue was extracted with pentane. Concentration under reduced pressure followed by cooling at -36°C gave **3** as blue crystals (67 mg, 0.063 mmol, 67% yield). Similar reaction of the pyridine adduct **2a** afforded **3** in 64% yield. IR 3718 (ν_{OH}), 2540 cm^{-1} (ν_{BH}). Anal. Calcd. for $\text{C}_{54}\text{H}_{94}\text{N}_{12}\text{O}_2\text{B}_2\text{Cr}_2$: C, 60.67; H, 8.86; N, 15.73. Found: C, 60.23; H, 8.68; N, 15.04%.

Reaction of **2b** with NaOH: formation of $\text{Tp}^{\text{iPr}_2}\text{Cr}(\mu\text{-OH})_2(\mu\text{-pz}^{\text{iPr}_2})\text{CrTp}^{\text{iPr}_2}$ **4**

To a methanolic solution (20 mL) of **2b** (230 mg, 0.326 mmol) was added an aqueous NaOH solution (1.5 M, 5 mL). Then the volatiles were removed under reduced pressure and the residue was extracted with pentane. Concentration under reduced pressure followed by cooling at -36°C gave **4** as blue crystals (67 mg, 0.063 mmol, 67% yield). IR 3685 (ν_{OH}), 2537 cm^{-1} (ν_{BH}). Despite several attempts an analytically pure sample could not be obtained.

Reaction of **3** with PhCH_2Cl : formation of $\text{Tp}^{\text{iPr}_2}\text{Cr}(\mu\text{-OH})_3\text{-CrTp}^{\text{iPr}_2}(\text{Cl})$ **5**

A mixture of **3** (238 mg, 0.223 mmol) and benzyl chloride (54 mL, 0.469 mmol) dissolved in toluene was stirred for one week at ambient temperature. Removal of the volatiles followed by crystallization from THF–MeCN gave **5** as red crystals (86 mg, 0.076 mmol, 34% yield). IR 3743 (ν_{OH}), 2551 (ν_{BH} for $\kappa^3\text{-Tp}^{\text{iPr}_2}$), 2471 cm^{-1} (ν_{BH} for $\kappa^2\text{-Tp}^{\text{iPr}_2}$). FD-MS: 1121 (M^+). Anal. Calcd. for $\text{C}_{54}\text{H}_{95}\text{N}_{12}\text{O}_3\text{B}_2\text{ClCr}_2$: C, 57.83; H, 8.54; N, 14.99. Found: C, 58.02; H, 8.44; N, 14.65%.

Reaction of **3** with O_2

Exposure of an ethereal solution (20 mL) of **3** (188 mg, 0.177 mmol) to O_2 atmosphere at -78°C immediately caused color

change from blue to brown. After the mixture was stirred for 4 h the volatiles were evaporated and the residue was crystallized from pentane to give a mixture of products, which could not be further separated. Single crystals were picked up by hands and subjected to X-ray crystallography.

Reaction of **3** with H₂O₂: formation of Tp^{ipr₃}Cr(OH)₂(OH)₂ **10**

An ethereal solution (16 mL) containing **3** (152 mg, 0.132 mmol) and a spoonful of Na₂SO₄ (a dehydrating agent) was cooled at -78 °C. Then an aqueous H₂O₂ solution (30%, 15 µL) was added to the mixture. The mixture was gradually warmed to 0 °C, when the color of the mixture changed from blue to red-brown. Filtration followed by cooling at -30 °C gave **10** as red crystals (66 mg, 0.116 mmol, 41% yield). IR 3668 (ν_{OH}), 2540 (ν_{BH}), 1645 cm⁻¹ (δ_{OH₂}). FD-MS: 1139 (M⁺ for **10**₂). Anal. Calcd. for C₂₇H₅₄N₆O₃BCr: C, 56.94; H, 8.85; N, 14.76. Found: C, 57.08; H, 8.52; N, 14.48%.

Reaction of **3** with Bu'OOH: formation of [Tp^{ipr₃}Cr(OH)₂]₂ **11**

An ethereal solution (20 mL) containing **3** (196 mg, 0.183 mmol) and a spoonful of Na₂SO₄ (a dehydrating agent) was cooled at -78 °C. Then Bu'OOH (70% Bu'OObu' solution, 47 µL, 0.38 mmol) was added to the mixture. Work up as described for **10** gave a trace amount of single crystals of **11**. IR 3656 (ν_{OH}), 2545 (ν_{BH} for κ³-Tp^{ipr₃}), 2484 cm⁻¹ (ν_{BH} for κ²-Tp^{ipr₃}).

Reaction of **10** with H₂O₂: synthesis of Tp^{ipr₃}Cr(O₂)₂ **12**

An ethereal solution (20 mL) containing **10** (333 mg, 0.585 mmol) and a spoonful of Na₂SO₄ (a dehydrating agent) was cooled at -78 °C. Then an aqueous H₂O₂ solution (30%, 2.2 mL, 14 mmol) was added to the mixture. The mixture was gradually warmed to 0 °C, when the color of the mixture changed from blue to red-brown. Filtration followed by cooling at -30 °C gave **12** as green solid (93 mg, 0.16 mmol, 27% yield). IR 3668 (ν_{OH}), 2552 (ν_{BH}), 945, 888 cm⁻¹ (ν_{OO}). Anal. Calcd. for C₂₇H₄₆N₆O₄BCr: C, 55.76; H, 7.97; N, 14.46. Found: C, 55.81; H, 8.07; N, 14.16. Treatment with H₂¹⁸O₂ gave the labeled compound Tp^{ipr₃}Cr(¹⁸O₂)₂ **12**-¹⁸O₂.

Isotope exchange reactions of **12**

To an ethereal solution (5 mL) of **12** (ca. 15 mg, 0.03 mmol) cooled at 0 °C was added aqueous H₂¹⁸O₂ solution (0.7 M, 0.5 mL, 0.35 mmol) or H₂¹⁸O (0.2 mL) and the resultant mixture was stirred for 20 min at the same temperature. Removal of the aqueous layer and drying with Na₂SO₄ followed by evaporation under reduced pressure gave green solid, which was analyzed by IR and FD-MS.

Spontaneous decomposition of **12**

An ethereal solution (40 mL) of **12** (507 mg, 0.87 mmol) prepared at 0 °C was stirred at ambient temperature. The color of the solution changed from green to brown and stirring was continued for 4 h. Chromatographic separation (alumina) of the mixture gave small amounts of **8** (eluted with ethyl acetate) and **10** (eluted with methanol), which were identified by IR.

Oxidation of organic compounds

To a toluene solution of **12** cooled at -78 °C was added an organic substrate and the resultant mixture was gradually warmed to room temperature. Organic products were analyzed by GLC and GC-MS. In the case of the PPh₃ oxidation the yield of O=PPh₃ was also checked by ³¹P-NMR.

X-ray crystallography

Crystallographic data are summarized in Table 2. Single crystals of **3** (pentane), **4** (MeCN), **5** (THF-MeCN), **7** (pentane), **9**

Table 2 Crystallographic data

Complex	3-2pentane	4-2MeCN	5	7-3pentane	9-4pentane	10-2pentane	11-H-pz ^{ipr₃}
Formula	C ₆₄ H ₁₁₈ N ₁₂ O ₂ B ₂ -Cr ₂	C ₆₇ H ₁₁₄ N ₁₆ O ₂ B ₂ -Cr ₂	C ₅₄ H ₉₅ N ₁₂ O ₃ B ₂ -ClCr ₂	C ₆₉ H ₁₃₄ N ₁₂ O ₈ B ₂ -Cr ₃	C ₇₄ H ₁₄₄ N ₁₂ O ₁₆ -B ₂ Cr ₆	C ₃₇ H ₇₄ N ₆ O ₃ BCr	C ₆₅ H ₁₁₂ N ₁₄ O ₄ -B ₂ Cr ₂
Formula weight	1213.33	1285.36	1121.49	1437.50	1791.62	713.84	1255.28
Crystal system	Triclinic	Triclinic	Triclinic	Triclinic	Monoclinic	Monoclinic	Triclinic
Space group	P1	P1	P1	P1	P2 ₁ /n	P2 ₁ /n	P1
a/Å	13.813(1)	14.7188(3)	13.621(1)	16.588(2)	11.7618(4)	13.1187(2)	15.6053(9)
b/Å	22.974(1)	21.615(1)	20.116(2)	18.845(2)	16.9666(3)	23.9459(8)	16.611(1)
c/Å	13.0204(4)	13.4270(8)	12.0553(8)	13.537(2)	24.6837(4)	13.5935(4)	14.3911(9)
α/°	101.495(4)	97.520(6)	97.853(6)	103.522(4)	90	90	99.328(2)
β/°	114.731(2)	102.367(3)	97.743(5)	100.57(1)	103.783(3)	92.537(1)	97.619(3)
γ/°	85.944(4)	108.213(4)	75.816(2)	90.225(6)	90	90	84.569(5)
V/Å ³	3677.3(3)	3872.4(4)	3154.8(4)	4039.7(8)	4784.0(2)	4266.1(2)	3638.4(4)
Z	2	2	2	2	2	4	2
μ/mm ⁻¹	0.342	0.329	0.435	0.452	0.719	0.307	0.350
R ₁ [I > 2σ(I)]	0.0943	0.0752	0.0638	0.0878	0.0895	0.0760	0.0719
wR ₂ (for all data)	0.2356	0.1999	0.1755	0.2410	0.2583	0.2406	0.1883

(pentane), **10** (pentane), **11** (ether) were obtained by recrystallization from the solvent systems shown in the parentheses and mounted on glass fibers.

Diffraction measurements were made on a Rigaku RAXIS IV imaging plate area detector with Mo K α radiation ($\lambda = 0.71069 \text{ \AA}$) at $-60 \text{ }^\circ\text{C}$. Indexing was performed from two oscillation images, which were exposed for 5 min. The crystal-to-detector distance was 110 mm ($2\theta_{\text{max}} = 55^\circ$). Neutral scattering factors were obtained from the standard source. In the reduction of data, Lorentz and polarization corrections and empirical absorption corrections were made.²¹ Crystallographic data and results of structure refinements are listed in Table 2.

The structural analysis was performed on an IRIS O2 computer using teXsan structure solving program system obtained from the Rigaku Corp., Tokyo, Japan.²² Neutral scattering factors were obtained from the standard source.²³

The structures were solved by a combination of the direct methods (SHELXS-86²⁴ or SIR92)²⁵ and Fourier synthesis (DIRDIF94).²⁶ Least-squares refinements were carried out using SHELXL-97²⁴ (refined on F^2) linked to teXsan. Unless otherwise stated all non-hydrogen atoms were refined anisotropically and methyl hydrogen atoms of the Tp^{ipr} ligand were refined using riding models and other hydrogen atoms were fixed at the calculated positions. Details of the refinements were as follows. **3**: OH hydrogen atoms were found by difference Fourier synthesis and fixed. Hydrogen atoms attached to one of the two pentane solvate with large B values are not included in the refinement. **4**: The MeCN solvates were refined isotropically. **5**: The OH hydrogen atoms were refined isotropically. **7**: During the refinement it was found that the CrO₂ bridge was disordered on two sites; one between O1 and O4 and the other between O2 and O5. The occupancy was refined to be Cr3O7O8 : Cr3AO7AO8A = 0.81 : 0.19. The minor components for the O1 and O4 moieties could not be located due to the low occupancy and therefore were not included in the refinement. The OH hydrogen atoms were fixed and the OH hydrogen atom associated with the O2 \cdots O5 bridge was not included due to the disorder problem. **9**: pentane solvates were refined isotropically and hydrogen atoms attached to the pentane solvate and the aquo ligand were not included in the refinement. **10**: The OH hydrogen atoms initially refined isotropically were fixed at the final stage of the refinement because of their rather large shift/error values. **11**: The disordered C76 atoms were refined taking into account minor component (C76 : C76A = 0.6 : 0.4) and hydrogen atoms attached to the disordered part were not included in the refinement. The OH and NH atoms initially refined isotropically were fixed at the final stage of the refinement because of their rather large shift/error values.

CCDC reference numbers 217496–217502.

See <http://www.rsc.org/suppdata/dt/b3/b309762e/> for crystallographic data in CIF or other electronic format.

Acknowledgements

We are grateful to the Ministry of Education, Culture, Sports, Science and Technology of the Japanese Government for financial support of this research (Grant-in-Aid for Scientific Research on Priority Areas: 11228201). We are also grateful to Professor Akihito Wada of our research laboratory for the measurements of Raman spectra of **12**.

References

- 1 R. A. Sheldon and J. K. Kochi, *Metal-Catalyzed Oxidations of Organic Compounds*, Academic Press, New York, 1981; S. Patai, *The chemistry of peroxides*, John Wiley & Sons, Chichester, 1983; A. E. Martel and D. T. Sawyer, *Oxygen Complexes and Oxygen Activation by Transition Metals*, Plenum Press, New York, 1988; W. Ando, *Organic Peroxides*, John Wiley and Sons, Chichester, 1992; thematic issue of Chem. Rev. (Metal-Dioxygen Complexes), *Chem. Rev.*, 1994, **94**, 567; G. Strukul, *Angew. Chem., Int. Ed.*, 1998, **37**, 1198.
- 2 M. Akita and S. Hikichi, *Bull. Chem. Soc. Jpn.*, 2002, **75**, 1657.
- 3 S. Trofimenko, *Scorpionates. The Coordination Chemistry of Polypyrazolylborate Ligands*, Imperial College Press, London, 1999.
- 4 Abbreviations used in this paper: Tp^R – hydrotris(pyrazolyl)borato ligands; Tp^{ipr} – 3,5-diisopropylpyrazolyl derivative; Tp^{bu,Me} – 3-*t*-butyl-5-methylpyrazolyl derivative; pz^R – pyrazolyl group.
- 5 M. Kosugi, S. Hikichi, M. Akita and Y. Moro-oka, *Inorg. Chem.*, 1999, **38**, 2567; M. Kosugi, S. Hikichi, M. Akita and Y. Moro-oka, *J. Chem. Soc., Dalton Trans.*, 1999, 1369.
- 6 K. Sugawara, S. Hikichi and M. Akita, *J. Chem. Soc., Dalton Trans.*, 2002, 4514.
- 7 The chemistry of peroxochromium species has not been studied in a systematic manner except for Stomberg's extensive structural studies in the 1960s. M. H. Dickman and M. T. Pope, *Chem. Rev.*, 1994, **94**, 569; R. Stomberg and C. Brosset, *Acta Chem. Scand.*, 1960, **14**, 441; R. Stomberg, *Nature*, 1962, **196**, 570; R. Stomberg, *Acta Chem. Scand.*, 1963, **17**, 1563; R. Stomberg, *Nature*, 1964, **201**, 486; R. Stomberg, *Ark. Kemi*, 1964, **22**, 29; R. Stomberg, *Ark. Kemi*, 1964, **22**, 49; R. Stomberg, *Nature*, 1965, **207**, 76; R. Stomberg, *Ark. Kemi*, 1965, **24**, 111; R. Stomberg, *Ark. Kemi*, 1965, **24**, 47; R. Stomberg and I. B. Ainalem, *Acta Chem. Scand.*, 1968, **22**, 1439; H. Mimoun, L. Saussine, E. Daire, M. Postel, J. Fisher and R. Weiss, *J. Am. Chem. Soc.*, 1983, **105**, 3101; E. Daire, H. Mimoun and L. Saussine, *Nouv. J. Chim.*, 1984, **8**, 271; H. Firouzabadi, N. Iranpoor, F. Kiaeezadeh and J. Toofan, *Tetrahedron*, 1986, **42**, 719; R. Curci, L. Lopez, L. Troisi, S. M. K. Rashid and A. P. Schaap, *Tetrahedron Lett.*, 1988, **29**, 3145; D. A. House and C. S. Garner, *Nature*, 1965, **20**, 776; R. H. A. Santos and M. T. P. Gambardella, *Polyhedron*, 1992, **11**, 799; M. T. H. Tarafder, P. Bhattacharee and A. K. Sarker, *Polyhedron*, 1993, **11**, 795.
- 8 (a) J. L. Kersten, R. R. Kucharczyk, G. P. A. Yap, A. L. Rheingold and K. H. Theopold, *Chem. Eur. J.*, 1997, **3**, 1668; (b) K. H. Theopold, *Eur. J. Inorg. Chem.*, 1998, 15; (c) A. Hess, M. R. Hörz, L. M. Liable-Sands, D. C. Lindner, A. L. Rheingold and K. H. Theopold, *Angew. Chem., Int. Ed.*, 1999, **38**, 166; (d) K. Qin, C. D. Incarvito, A. L. Rheingold and K. H. Theopold, *Angew. Chem., Int. Ed.*, 2002, **41**, 2333; (e) K. Qin, C. D. Incarvito, A. L. Rheingold and K. H. Theopold, *J. Am. Chem. Soc.*, 2002, **124**, 14008; (f) See also J. S. Hess, S. Leelasubcharoen, A. L. Rheingold, D. J. Doren and K. H. Theopold, *J. Am. Chem. Soc.*, 2002, **124**, 2454.
- 9 H. E. Bryndza and W. Tam, *Chem. Rev.*, 1988, **88**, 1163; F. Bottomley and L. Sutin, *Adv. Organomet. Chem.*, 1988, **28**, 339.
- 10 The structure of Tp^{ipr}Cr(μ -OMe)₂Cr(μ -OMe)₂CrTp^{ipr} [IR(KBr) 2809 ($\nu_{\text{CH}}(\text{OMe})$), 2539 cm^{-1} (ν_{BH})] was confirmed by X-ray crystallography but could not be refined satisfactorily owing to the insufficient number of diffraction data. Cell parameters for Tp^{ipr}Cr(μ -OMe)₂Cr(μ -OMe)₂CrTp^{ipr}·2pentane: monoclinic, $C2/c$, $Z = 4$, $a = 25.905(4) \text{ \AA}$, $b = 16.603(3) \text{ \AA}$, $c = 19.437(2) \text{ \AA}$, $\beta = 100.429(8)^\circ$, $V = 8222(2) \text{ \AA}^3$.
- 11 (a) H. Komatsuzaki, S. Hikichi, M. Akita and Y. Moro-oka, *Inorg. Chem.*, 1998, **37**, 3652; (b) Y. Takahashi, M. Hashimoto, S. Hikichi, M. Akita and Y. Moro-oka, *Angew. Chem., Int. Ed.*, 1999, **38**, 3074; (c) S. Hikichi, M. Yoshizawa, K. Uehara, and M. Akita, unpublished result.
- 12 (a) A. W. Addison, T. N. Rao, J. Reedijk, J. van Rijn and G. C. Verschoor, *J. Chem. Soc., Dalton Trans.*, 1984, 1349; (b) See also S. Alvarez and M. Llundell, *J. Chem. Soc., Dalton Trans.*, 2000, 3288.
- 13 (μ -OH)(μ -OAc)(CrTp^{ipr})₂ was obtained as a mixture with the di- μ -acetato complex, (μ -OAc)₂(CrTp^{ipr})₂. Although single crystals were separated manually, analytically pure samples could not be obtained. (μ -OH)(μ -OAc)(CrTp^{ipr})₂: IR(KBr) 3663 (ν_{OH}), 2542 (ν_{BH}), 1577 cm^{-1} ($\nu_{\text{C-O}}$); cell parameters: monoclinic, $P2_1/c$, $Z = 4$, $a = 19.657(6) \text{ \AA}$, $b = 12.854(4) \text{ \AA}$, $c = 22.885(6) \text{ \AA}$, $\beta = 99.130(2)^\circ$, $V = 6703(3) \text{ \AA}^3$. (μ -OAc)₂(CrTp^{ipr})₂: IR(KBr) 2535 (ν_{BH}), 1607 cm^{-1} ($\nu_{\text{C-O}}$).
- 14 M. Akita, K. Ohta, Y. Takahashi, S. Hikichi and Y. Moro-oka, *Organometallics*, 1997, **16**, 4121.
- 15 H. Komatsuzaki, Y. Nagasu, K. Suzuki, T. Shibasaki, M. Satou, F. Ebina, S. Hikichi, M. Akita and Y. Moro-oka, *J. Chem. Soc., Dalton Trans.*, 1998, 511; N. Kitajima, M. Osawa and Y. Moro-oka, *J. Am. Chem. Soc.*, 1991, **113**, 7757; M. Osawa, M. Tanaka, N. Kitajima and Y. Moro-oka, *J. Am. Chem. Soc.*, 1997, 919; M. Osawa, K. Fujisawa, N. Kitajima and Y. Moro-oka, *Chem. Lett.*, 1991, **113**, 7757.
- 16 For dinuclear μ -peroxo intermediates, see N. Kitajima, N. Tamura, H. Amagai, H. Fukui, Y. Moro-oka, Y. Mizutani, T. Kitagawa, R. Mathur, K. Heerwegh, C. A. Reed, C. R. Randall, L. Que, Jr. and K. Tatsumi, *J. Am. Chem. Soc.*, 1994, **116**, 9071; K. Kim and S. J. Lippard, *J. Am. Chem. Soc.*, 1996, **118**, 4914. See also ref. 15.

- 17 The structure of complex **8** was confirmed by X-ray crystallography but could not be refined satisfactorily owing to the insufficient number of diffraction data. Cell parameters for **8**·2pentane: orthorhombic, *Pccn*, $Z = 4$, $a = 21.718(2)$, $b = 22.639(3)$, $c = 17.273(2)$ Å, $V = 8493(2)$ Å³.
- 18 Cyclic μ -chromato or -dichromato complexes have a few precedents. See for example P. Chaudhuri, M. Winter, K. Wieghardt, S. Gehring, W. Haase, B. Nuber and J. Weiss, *Inorg. Chem.*, 1988, **27**, 1564; S. Druke, K. Wieghardt, B. Nuber, J. Weiss, H.-P. Fleischhauer, S. Gehring and W. Haase, *J. Am. Chem. Soc.*, 1989, **111**, 8622; R. C. Y. Bruggemann and U. Thewalt, *Z. Naturforsch., B*, 1994, **49**, 1531; B. C. Dave and R. S. Czernuszewicz, *Inorg. Chem.*, 1994, **33**, 847; G. D. Munno, T. Poerio, M. Julve, F. Lloret, J. Faus and A. Caneschi, *J. Chem. Soc., Dalton Trans.*, 1998, 1679.
- 19 Y. Takahashi, M. Akita, S. Hikichi and Y. Moro-oka, *Inorg. Chem.*, 1998, **37**, 3186; Y. Takahashi, S. Hikichi, Y. Moro-oka and M. Akita, *Polyhedron*, in the press.
- 20 The two $\nu_{\text{O-O}}$ absorptions should result from symmetric and antisymmetric coupling of the two O–O parts. Separation of O–O vibrations was noted for some diperoxo-chromium(IV) complexes.
- D. A. House, R. G. Hughs and C. S. Garner, *Inorg. Chem.*, 1967, **6**, 1077.
- 21 T. Higashi, *Program for absorption correction*, Rigaku Corp., Tokyo, Japan, 1995.
- 22 teXsan, Crystal Structure Analysis Package, ver. 1. 11, Rigaku Corp., Tokyo, Japan, 2000.
- 23 *International Tables for X-ray Crystallography*, Kynoch Press, Birmingham, 1975, vol. 4.
- 24 (a) G. M. Sheldrick, SHELXS-86, Program for crystal structure determination, University of Göttingen, Germany, 1986; (b) G. M. Sheldrick, SHELXL-97, Program for refinement of crystal structures, University of Göttingen, Germany, 1997.
- 25 A. Altomare, M. C. Burla, M. Camalli, M. Cascarano, C. Giacovazzo, A. Guagliardi and G. Polidori, *J. Appl. Crystallogr.*, 1994, **27**, 435.
- 26 P. T. Beurskens, G. Admiraal, G. Beurskens, W. P. Bosman, S. Garcia-Granda, R. O. Gould, J. M. M. Smits, and C. Smykalla, *The DIRDIF program system, Technical Report of the Crystallography Laboratory*, University of Nijmegen, Nijmegen, The Netherlands, 1992.